

Occlusion-aware Risk Assessment and Driving Strategy for Autonomous Vehicles Using Simplified Reachability Quantification

Hyunwoo Park¹, Jongseo Choi¹, Hyuntai Chin¹, Sang-Hyun Lee² and Doosan Baek^{1,2*}

Abstract—There are several unresolved challenges for autonomous vehicles. One of them is safely navigating among occluded pedestrians and vehicles. Previous works solved this problem by generating phantom cars and assessing their risk. However, few of them solved the problem effectively. Some of them over-approximate the phantom cars and made the ego vehicle overly conservative, and some of them assess the risk of unnecessary phantom cars and cannot keep in real-time in heavily occluded situations. In this paper, motivated by the previous works, we propose an algorithm that efficiently assesses risks of phantom pedestrians/vehicles using *Simplified Reachability Quantification*. We utilized this occlusion risk to set a speed limit at the risky position when planning the velocity profile of an autonomous vehicle. This allows an autonomous vehicle to safely and efficiently drive in occluded areas. The proposed algorithm was evaluated in various scenarios in the CARLA simulator where occlusion presents due to stopping cars and obstacles. Our method reduced the average collision rate by $6.14\times$, the discomfort score by $5.03\times$, while traversal time was increased by $1.48\times$ compared to baseline 1, and computation time was reduced by $20.15\times$ compared to baseline 2.

Index terms—Autonomous Vehicle, Occlusion, Risk Assessment, Motion Planning

I. INTRODUCTION

LiDARs, cameras, and radars are often used in autonomous vehicles and other mobile robots to perceive surroundings. But due to their nature of line-of-sight trait, they have a critical disadvantage under occlusion in common situations like Fig.1. When occlusion is present in the scene, there could be potentially dangerous situations where traffic participants who were in the occluded area may come out from it and move into the driving corridor [1], [2]. Human drivers could safely drive under occlusion by decreasing velocity depending on the extent of occlusion and its riskiness, yet not losing efficiency.

Autonomous vehicles must also assess the potential risks due to occlusion and its extent of risk. Previous works solved this problem by generating hypothetical agents called Phantom Agent(PA) in the occluded region. In [3], they proposed a set-based prediction that contains every possible future behavior of PAs. However, they didn't quantify the occlusion risk, which could make the ego vehicle overly conservative. In [4], [5], they quantify the occlusion risk by

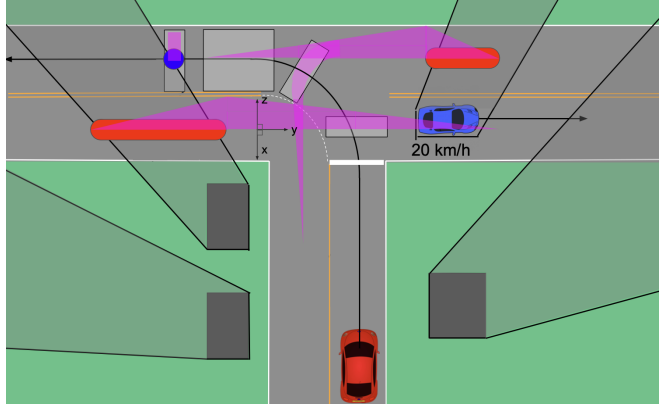


Fig. 1: The ego vehicle(red vehicle) is entering the intersection. Occlusion due to an obstacle(gray) and another car(blue vehicle) is represented as a gray-shaded region. The position of hidden vehicles that have the potential to make a collision with the ego vehicle are illustrated in red and blue points. The blue one has the same direction as the ego vehicle and the reds are not. The risk due to hidden agents is represented as magenta along the road on the z-axis. The riskier it is the higher it gets. The region along the route path that has occlusion risk is represented as a gray rectangle.

sampling the particles which represent PAs in the occluded area. However, in heavily occluded areas, sampling the particles of the occluded area gets impossible to keep in real-time due to intensive computation.

This paper presents a novel algorithm that quantifies the risk of occluded traffic agents and a planning strategy that safely navigates through occluded regions using it. First, we generate PAs in occluded regions that have the ability to affect the ego vehicle. Second, we quantify the risk of the PAs. Third, using the occlusion risk we derived, we develop a driving strategy that makes the ego vehicle to drive safe and comfortable. Our algorithm is robust against various driving environments with various types of traffic participants including pedestrians. Also by using *Simplified Reachability Quantification* which quantifies the risk of phantom vehicles considering the road network, occlusion risk is computed in constant time which made our method work in real-time even in heavily occluded real road situations. An experiment of comparison of w/ and w/o our algorithm was done using the CARLA simulator where occlusion presents due to stopping cars and obstacles. We decreased the collision rate by $6.14\times$ and discomfort score by $5.03\times$ while the total computation time of the planning stack was reduced by $20.15\times$ compared to state-of-the-art algorithm [5].

The main contributions of our method are as follows:

- We present an algorithm that is robust against various driving environments with various types of traffic par-

¹ ThorDrive, Seoul, 07268, Republic of Korea
 {hwpark, jschoi, htchin, dsbaek}@thordrive.ai

² Seoul National University, Seoul, Republic of Korea
 slee01@snu.ac.kr

* Corresponding author

ticipants including pedestrians.

- We validate our algorithm in various types of occluded scenarios in the CARLA simulator. Our method resulted in a remarkable decrease in ride discomfort and collision rate.
- We introduce the *Simplified Reachability Quantification*, which computes occlusion risk in constant time and made our algorithm work in real-time even in heavily occluded real road situations.

The remainder of the paper is organized as follows: Section II reviews related works of occlusion risk assessment and driving strategy utilizing it. Section III defines terms and concepts which would be used in later sections. Section IV describes how our method finds phantom agents that are relevant to the route path of the ego vehicle and assess their risk to utilize for motion planning. Section V shows how our method is evaluated in the CARLA simulator and introduces baseline algorithms to compare. Section VI analyzes the evaluation results and shows how the key metrics are improved. Section VII concludes the proposed method and discusses future works.

II. RELATED WORK

Most of the previous works could be classified by following two categories: *Probabilistic based methods* [4]–[8], and *Over-approximating methods* [3], [9], [10]. There are also other kinds of methods variated from two methods, recreated itself by using concepts like *Sequential Reasoning* [10], [11]. On the following paragraphs, a brief explanation of occlusion risk assessment methods, its limitation, and driving strategies using them will be described by category.

Probabilistic Methods: Probabilistic methods assess an occlusion risk by formulating the problem probabilistically. They quantify the occlusion risk of each point. In [5], they sampled the *potential vehicles*’ predicted positions to assess occlusion risk however they didn’t consider the type of the *potential vehicles* to filter out the unnecessary ones, and the particles during the prediction horizon. Sampling each and every particle was also inefficient. Whereas our approach covers mentioned limits and efficiently generates a distribution of the *potential vehicles* within the prediction horizon. In [4], they calculated **BRS**(Backward Reachability Set) of every particle of **FRS**(Forward Reachability Set) of the ego-vehicle to assess occlusion risk which could be inefficient when the number of the particle gets large. Also, they consider every possible control input of the *potential vehicles* which is inefficient since most of the vehicles drive along the lane.

Over-approximating Methods: Over-approximating methods could be seen as a special case of probability-based methods [4], [5] where the probability of every small risk is considered as 100%. In [3], *edge*(first introduced by [9]) was used to classify *static* and *dynamic* phantom vehicles. It made it possible to assess occlusion risk according to the result of the classification of *phantom vehicle* which was more efficient. Due to its nature, over-approximating

methods are efficient, yet it tends to make the ego vehicle conservative and even make it freeze in some corner cases where the ego vehicle must take a risk to pass through.

Sequential Reasoning: There were works that solve the occlusion problem by considering only necessary agents by reasoning observations over time. In [10], they used *over-approximating methods* to track the hidden agents conservatively over time and formulate the *p-safe*(passive-safety) [12] planning strategy using the concept **IBCS** [13] and **RSS** [14]. However, they tracked every possible agent over their sensor range which is hardly efficient in heavy occluded areas and when using long-range sensors.

Driving Strategies: Driving strategies differ from how the occlusion-aware risks are assessed. For probabilistic methods, [5] uses optimization to generate a trajectory with low occlusion risk, [8] selects a trajectory with a minimum cost function that includes occlusion risk term, and [6] slows down the velocity when risk is high enough before entering an intersection. For over-approximating methods, [3], [9] used fail-safe trajectory [15], [16] that are collision-free for any feasible control of other vehicles.

III. PRELIMINARIES

In this section, problem setting and primary concepts used in later sections will be defined. Let $t \in \mathbb{R}$ be time, the state of the system at time t as $x(t)$ in the Cartesian state space $\mathcal{X} \subset \mathbb{R}^2$ and the vehicle’s control input u in the action space $\mathcal{U} \subset \mathbb{R}^2$. The environment surrounding ego vehicle consists of $n \in \mathbb{Z}$ number of lanes $l \in L$. Each and every lane l has P^l which is set of *continuous* and *sequential* centerline points. The k -th lane l_k , where $(0 \leq k \leq n, k \in \mathbb{Z})$, has m number of centerline points $P^{l_k} = \{p_1^k, p_2^k, p_3^k, \dots, p_m^k\}$ in the Cartesian space $p \in P \subset \mathbb{R}^2$. The route path of the ego vehicle is predefined points following certain lanes $l \in L$ to reach the goal in the Cartesian space represented as $route(x(t_0)) = \{x(t_0), x(t_1), x(t_2), \dots, x(t_k)\}$ where $x(t) \in \mathcal{X}$.

Definition 1. (Observable Polygon, \mathbb{O}). \mathbb{O} is generated by vehicle’s light-of-sight sensors from ego vehicle. It consists of points p in the Cartesian space $p \in \mathbb{O} \subset \mathbb{R}^2$.

Definition 2. (Phantom Agent). Phantom Agent(PA) is a potentially hidden agent that its position is outside of the observable polygon and it is modeled as point mass models as [4], [5], [11] did. It is safer since small agents like cyclists and children could be included. PA is classified as a phantom vehicle(PV) or a phantom pedestrian(PP).

PVs are assumed to be always on the road and following center of lane. They could have various velocity(even exceeding the speed limit of the road). Unlike PVs, PPs could be anywhere since they don’t get physically constrained like cars in sidewalk. In [10], they also introduced *illegally behaving pedestrians* that walks on road.

Definition 3. (Forward Reachable Set, **FRS)**

Given initial state x_0 at time t_0 and fixed time horizon T_{fix} , the FRS is a set of states that could be reached in given time

horizon starting from initial state and it is defined as follows:

$$FRS(x_0, T_{fix}) := \{x(t) \in \mathcal{X} | \dot{x}(t) = u(t), \forall u(t) \in \mathbb{U}, \forall t \in [t_0, t_0 + T_{fix}]\} \quad (1)$$

Definition 4. (Backward Reachable Set, BRS)

Given final state x_f at time T_{fix} where T_{fix} is fixed time horizon, the BRS is a set of initial states at time t_0 that could reach the x_f in given time horizon and it is defined as follows:

$$BRS(x_f, T_{fix}) := \{x_0 \in \mathcal{X} | x_f \in FRS(x_0, T_{fix}), \forall t \in [t_0, t_0 + T_{fix}]\} \quad (2)$$

IV. METHOD

We first generate PAs in the occluded region. This step consists of *Node Classification*(IV-A) and *Inferring Phantom Agent Zone*(IV-B). *Node Classification* outlines the positions of PAs using road situations and occluded area, *Inferring Phantom Agent Zone* finds every position of PAs that have the ability to affect the ego vehicle. Second, we define occlusion risk by quantifying the risk of the PAs using *Simplified Reachability Quantification*(IV-C). Third, using the occlusion risk we derived, we develop a driving strategy by setting a speed limit for the ego vehicle where occlusion risk presents.

A. Node Classification

The potential positions of PVs are points on the centerlines of lanes P^{l_k} in the occluded area. However, considering every PV is inefficient. We could efficiently assess risk by classifying PV, whether the PV would *statically* or *dynamically* risk the ego vehicle [9], and by removing PVs that can't reach the route of the ego vehicle in the prediction horizon T_{pred} . The above efficiency is achieved, by a sequence of procedures consisting of *Node Classification* and *Inferring Phantom Agent Zone*. *Node Classification* is a cornerstone of the procedure to achieve efficiency. The result of it is used for the *Inferring Phantom Agent Zone* by a search starting from each node. The illustration of *Node Classification* is in Fig.2 (a)-(c) and it consists as follows:

1) The Intersection of Observable Polygon and lanes:

First, *intersected Nodes* \mathbb{I} is defined as intersection of \mathbb{O} and centerline of lanes P^{l_k} . *Intersected Nodes* are used for finding out potential positions of PVs and we only need the centerline of lanes P^{l_k} to assess the risk of every PV. (Detailed explanations are in IV-C.1, IV-C.2). However, we exclude the intersected points which overlap with other vehicles or are too close to other vehicles. Since the positions of PVs inferred intersected points will be so small or overlap with objects that even small agents can't exist.

$$\mathbb{I} = \{p \in \mathbb{R}^2 | p = \mathbb{O} \cap P^{l_k}, k \in \{1, 2, 3, \dots, m\}\} \quad (3)$$

2) *Static/Dynamic Node Classification*: Second, we classify \mathbb{I} into static node \mathbb{S} and dynamic node \mathbb{D} . The static/dynamic node came from static/dynamic edges in [3]. They named it static edge since they over-approximate PVs and the riskiest move the PV generated from static edge

could have is stopping in front of PV. However we modified it since we don't over-approximate the shape of the PV and we need an interval to find every possible position of PVs, not over-approximating by using an edge. We first classify the \mathbb{I} as \mathbb{S} , if \mathbb{I} has any intersection with $FRS(x_{ego}, T_{fix})$. Then the rest of the \mathbb{I} is \mathbb{D} . Static nodes can be visited by the ego vehicle in a given fixed time horizon and dynamic nodes can't be visited. This property makes inferring positions of PVs and risk assessment efficient.

$$\begin{aligned} \mathbb{S} &= FRS(x_{ego}, T_{fix}) \cap \mathbb{I}, \\ \mathbb{D} &= \mathbb{I} - \mathbb{S} \end{aligned} \quad (4)$$

3) *Relevant/Irrelevant Node Classification*: Before inferring the positions of the PVs using static/dynamic nodes, we have to classify whether the node is necessary or not. There are unnecessary nodes that don't have to be considered because their FRS doesn't collide with *route path* of the ego vehicle in T_{pred} . We define a node as a *Relevant Node* \mathbb{RN} if $FRS(i, T_{pred})$ where $i \in \mathbb{I}$ collides with the route path of the ego vehicle and as *Irrelevant Node* \mathbb{IN} if it doesn't. However if the $i \in \mathbb{S}$, we only consider the first \mathbb{S} that is reached by the route path of the ego vehicle as a *relevant* like [3] did. Since *static* occlusion risk by other \mathbb{S} are already taken care of by the first one. Note that the concept *relevant* will be used to characterize other terms as a trait in the following sections.

$$\begin{aligned} \mathbb{RN} &= \{i \in \mathbb{I} | FRS(i, T_{pred}) \cap route(x(t_0)) \neq \emptyset\} \\ \mathbb{IN} &= \{i \in \mathbb{I} | FRS(i, T_{pred}) \cap route(x(t_0)) = \emptyset\} \end{aligned} \quad (5)$$

B. Inferring Phantom Agent Zone

Phantom Agent Zone is a set of occluded points where *relevant* agents exist. It is consists of *Phantom Vehicle Zone*(PVZ) and *Phantom Pedestrian Zone*(PPZ). PVZ consists of *Phantom Vehicle Set*(PVS) which is a set of occluded points in a lane that are continuously connected to each other. We assume that there is one *relevant* PV exists in every PVS which makes every PVS includes at least one *Relevant Node*. If a PVS includes a *relevant* \mathbb{D} , it is defined as *Dynamic* PVS, however, if it includes *relevant* \mathbb{S} , then *relevant* \mathbb{S} alone is defined as *Static* PVS. In Fig.2d, Dynamic PVS is represented as a red line and Static PVS is represented as a blue dot. For every point in occluded area $p \in \mathbb{O}^c$ and every link l_k , PVZ is defined as follows:

$$PVZ := \{p \in P^{l_k} | FRS(p, T_{pred}) \cap route(x(t_0)) \neq \emptyset\} \quad (6)$$

In the following subsections, why we chose *relevant* \mathbb{S} as a Static PVS and algorithm description finding Dynamic PVS using *Relevant* \mathbb{D} will be explained.

1) *Static Phantom Vehicle Set*: Defining positions of every PV that *statically* risk the ego vehicle as Static PVS is dangerous and inefficient. If we found every PV and assess its risk(details are in IV-C), it would be riskier since occlusion risk would be scattered. Also, we observed that static occlusion risk is often removed before it affects the ego vehicle. This characteristic of static occlusion risk makes defining every PV as Static PVS unnecessary and also

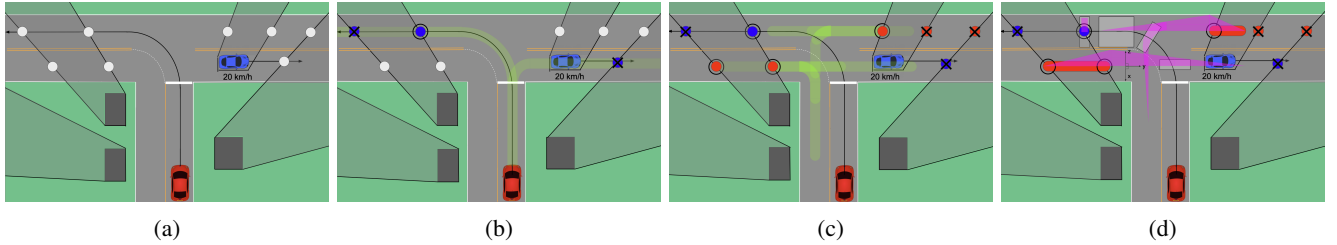


Fig. 2: Illustration of our algorithm. The ego vehicle(red vehicle) is navigating through an intersection with the occluded area(gray shaded area) while the other vehicle(blue vehicle) is passing through. (a) Intersected nodes are represented as white points. (b) Relevant static node(blue point inside a circle), and irrelevant static nodes(blue point with X mark) are classified using the FRS of the ego vehicle(yellow shaded region). (c) Relevant dynamic nodes(red points inside circle) and irrelevant dynamic nodes(red points with an X mark) are classified using the FRS(yellow region) of dynamic nodes.

prevents the ego vehicle from conservative movement even if we define *Relevant S* as Static PVS which is the most dangerous assumption for the ego vehicle. Therefore defining Static PVS as *Relevant S* is an efficient and safest way to consider the positions of *Static PVs*.

2) *Dynamic Phantom Vehicle Set*: Dynamic PVS could be found by following steps: (1) The starting point of Dynamic PVS is *Dynamic Relevant Node*. (2) In the reverse direction of the lane, new point p_{new} is added to Dynamic PVS from starting point until (3),(4) occurs. (3) If p_{new} gets in to the \mathbb{O} , it stops. (4) If $FRS(p_{new}, T_{pred})$ doesn't collide with the route path of the ego vehicle, it stops. Dynamic PVS in a common intersection scenario is shown in Fig.3. Using Dynamic PVS, Every potential *dynamic PV* that is *relevant* with the ego vehicle is considered.

3) *Phantom Pedestrian Zone*: Unlike PV, PP could be anywhere. In [10], they called PP who are outside of a sidewalk or on a crosswalk, a *illegally-behaving pedestrians*. Since a region of illegally behaving pedestrians covers a region of legally behaving pedestrians, we only consider illegally behaving pedestrians. Given T_{pred} and the x_k which is an element of the route path of the ego vehicle, PPZ is defined as follows:

$$\text{PPZ} := \{p \in \mathbb{O}^c\} \cap BRS(x_k, T_{pred}) \quad (7)$$

Unlike PVZ, pedestrians could be anywhere and there aren't any nodes to use FRS, therefore BRS of the route path is used to find PPZ. The farthest PP(edge of the PPZ) from the route path of the ego vehicle would be PP which is moving at maximum speed toward reference through the shortest path. Therefore in a road like Fig.4, simply PPZ will be an area that subtracts an observable polygon from the rectangular area along the route path.

C. Risk Assessment

In this section, where the PVs and PPs would risk the ego vehicle and how risky it would be is found using *Phantom Agent Zone*.

1) *Static Phantom Vehicle*: For the same reason why we set Static PVS as a *Static Relevant Node*, we chose to assume that PV in Static PVS is stopping which is an efficient and most conservative way to assess its risk.

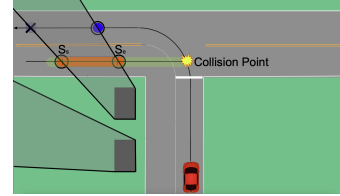


Fig. 3: The start position of dynamic phantom agent zone(red) is $(s_s, 0)$ and end position is $(s_e, 0)$ in the Frenet frame of PV. The BRS of a collision point is represented as a yellow-shaded area.

2) *Dynamic Phantom Vehicle*: Strongly motivated by [4], [5], we improved their occlusion risk assessment method computation-wise using the *Simplified Reachability Quantification*. The basic idea of assessing the risk of Dynamic PVS is as follows: Let prediction horizon T_{pred} that is inevitable or proximately impossible to avoid a collision with sudden appearing vehicles due to computation time of autonomous driving stack and let collision point a point of intersection between the route of the ego vehicle and FRS of a PV in T_{pred} . If an element of BRS of collision point in T_{pred} is in an occluded area, then there exists an occlusion risk due to the PV. It represents that there could be a PV in the occluded area that has the ability to cause a collision. It will be riskier if there are more elements of BRS included in the occluded area. We assume that PV is uniformly distributed along the Dynamic PVS and PV has a uniformly distributed velocity $[0, v_{max}]$ since we assume no prior information like [5] did. Also, we assume that PV moves at constant velocity for the same reason. Given T_{pred} , Dynamic PVS, and maximum velocity of PV v_{max} , we could quantify the occlusion risk $f(s)$ of the Dynamic PVS using *Simplified Reachability Quantification*. The start position of Dynamic PVS is s_s and the end position is s_e and its illustration is in Fig.3. Occlusion risk is illustrated in Fig.2d and defined as follows. Prove and I_1, I_2, I_3 , the domain of s , are in APPENDIX.

$$f(s)$$

$$:= \begin{cases} \frac{1}{2}(2v_{max} - \frac{s-s_s}{T_{pred}})(s - s_s), & s \in I_1 \\ \frac{1}{2}(2v_{max} - \frac{s-s_s}{T_{pred}} - \frac{s-s_e}{T_{pred}})(s_e - s_s), & s \in I_2 \\ \frac{1}{2}(v_{max} - \frac{s-s_e}{T_{pred}})(s_e - (s - v_{max}T_{pred})), & s \in I_3 \end{cases} \quad (8)$$

Eq.8 is considering every possible motion of PV in every position in Dynamic PVS without prior and it simply means if the $f(s)$ gets higher the ego vehicle gets riskier in the position s . However we assumed that PV is uniformly distributed in Dynamic PVS, in other words, we assumed that actual vehicle always exists in Dynamic PVS. The probability of the existence of an actual vehicle in Dynamic PVS should be considered as well. Naturally, there is more probability of the existence of an actual vehicle in Dynamic PVS if the Dynamic PVS is longer. Therefore the occlusion risk should be bigger if the Dynamic PVS is longer. The occlusion risk $o(s)$ considering the probability of the existence of an actual vehicle in Dynamic PVS is defined as follows:

$$o(s) := (s_e - s_s) \cdot f(s) \quad (9)$$

However, assessing the risk of Dynamic PVS of which collision point is too far from the ego vehicle is unnecessary. It is efficient to filter out the Dynamic PVS of which the collision point is farther than *Static Node* or farther than a certain distance proportional to the current velocity of the ego vehicle.

Since not every vehicle drives along the centerline of the road, we consider the lateral deviation of PVs. We believe that the lateral deviation of PV could be represented as a normal distribution of which the confidence interval of $p(90\%)$ is used in evaluation) is $[-\text{road_width}/2, \text{road_width}/2]$. Let $w(d) := N(0, (\frac{\text{road_width}}{2 \times \mathcal{Z}(1-0.5(1-p))})^2)$, then the final risk distribution per Dynamic PVS is defined as follows:

$$r(s, d) := o(s) \times w(d) \quad (10)$$

3) *Phantom Pedestrian*: Unlike PV, PP could move in any direction. So FRS of a PP given T_{pred} could be assumed as a circle. However, we don't have to consider the PP moving away from the route of the ego vehicle which makes the FRS of PP a shape of a half-circle toward the route path. Without prior information being given, we could assume the PP would move straight toward to closest way point of the route path. Since the expected heading angle of PP would be straightforward to the closest waypoint of the route path.

Assuming that the heading angle of PP is fixed, risk assessment for PP is the same as PV. Given $s_s, s_e, T_{pred}, v_{max}$, and using Eq.(9), we could assess occlusion risk due to PP. However, assessing the risk of PP too far from the current position is unnecessary. It is efficient to filter out the unnecessary PPs as we did in the risk assessment of PV. It is illustrated in Fig.4.

D. Driving Strategy

In this section, a driving strategy that ensures the safety of the ego vehicle from occlusion risk is made using the result of IV-C. There are lots of driving strategies for occlusion risk assessment. One could plan a trajectory that reduces an occlusion risk [4], [5], [8], or plan the velocity of a fixed path [6], [17]–[19]. We chose to plan the velocity of a fixed path. Since expert drivers rarely change a path(lateral deviation) in common occluded situations like intersections, roads with

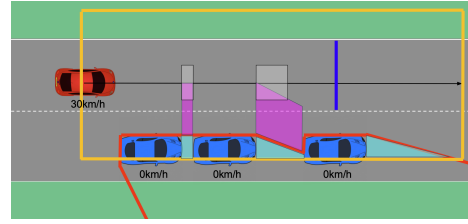


Fig. 4: The ego vehicle(red vehicle) is driving along street parking cars(blue vehicles). The PPZ(cyan) is derived from BRS(the area inside the yellow box) of the route path(black) and the observable polygon(red). Its risk is represented as magenta on the xy plane and the risk of PPs' after the blue line is filtered out.

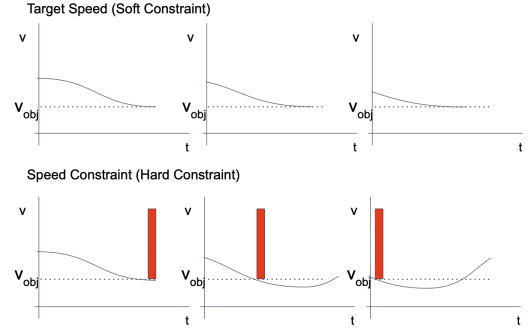


Fig. 5: Illustration of velocity planning delay. The same velocity has been given as the target speed and speed limit. The red square represents the speed limit due to occlusion risk.

street parking cars, and narrow alleys. Also, parameter tuning of with/without occlusion risk for trajectory generation is hard or even won't work in the desired way.

With occlusion risks from IV-C, there are few options to slow down the velocity of the ego vehicle on a fixed path. It could be directly used to (1) *cost function* of optimization or trajectory selection, (2) lower the *target velocity*, or (3) add a *speed limit* condition.

Directly using occlusion risks (1) as a potential field for optimization could yield a high computational load or even be infeasible since the occlusion risk distribution is spread over a large area. Lowering the target velocity (2) won't be effective if velocity planning is calculated in every time step. The time the ego vehicle reaches the target velocity will be delayed like Fig.5 [20]. Adding a speed limit (3) is an agile and effective approach that can be aware of an exact position and guarantees to slow down at the exact position. Also, it could be easily integrated with any planning algorithm by adding an extra constraint $v \leq v_{speed_limit}$ in the optimization process or selecting a trajectory that satisfies the speed limit from sampled trajectories.

1) *Speed Limit*: The speed limit v_{speed_limit} and its position p_{speed_limit} due to occlusion risk is defined as follows. First, find the points of the route path of the ego vehicle where occlusion risks exist. Second, cluster the points. Third, calculate the *weighted average* of those points by occlusion risk. Finally, the speed limit is defined as follows:

$$p_{speed_limit}^{[c]} := \sum_{k=1}^N \frac{r_k^{[c]} \cdot p_k^{[c]}}{r_{total}^{[c]}} \quad (11)$$

Where $c \in C$ is cluster of occlusion risk points, p_{speed_limit} is weighted average position of occlusion risk points per cluster c , N is number of points in cluster c , $r_{total}^{[c]}$ is total sum of occlusion risk defined in Eq.10 in cluster c .

$$v_{speed_limit}(r_{total}^{[c]}) = \begin{cases} v_{road_speed_limit}, & r_{total}^{[c]} \leq c_{th} \\ \frac{v_{occ_min} - v_{occ_max}}{1 - c_{th}} \times (r_{total}^{[c]} - c_{th}) \\ + v_{occ_max}, & r_{total}^{[c]} > c_{th} \end{cases} \quad (12)$$

where $v_{road_speed_limit}$ is the speed limit of the road, c_{th} is minimum occlusion risk threshold, v_{occ_min} , v_{occ_max} are minimum and maximum speed limit when there is an amount of occlusion risk worth to consider. v_{speed_limit} has simple linear relation. It is low when occlusion risks are high and vice versa. v_{occ_min} is for a risk-taking feature of the expert driver and also preventing the ego vehicle from freezing and never reaching the goal. If $c_{th} = 0$ and $v_{occ_min} = v_{occ_max} = 0$ then, our method gets similar to over-approximating methods.

2) Planning: We chose Piecewise-Jerk Speed Optimization(PJSO) method [21] for velocity planning. It minimizes cost function consisting of traversal time and ride comfort. We added the speed limit as a hard constraint of the optimization problem as follows:

$$\dot{x}(t) < \min(\sqrt{a_{lateral_max}/\kappa(x)_{max}}, v_{speed_limit}) \quad (13)$$

where $\kappa(x)_{max}$ is the maximum curvature of the ego vehicle and $a_{lateral_max}$ is maximum lateral acceleration along the fixed path, together $\sqrt{a_{lateral_max}/\kappa(x)_{max}}$ represents an approximate speed limit due to curvature of fixed path.

V. EVALUATION

We compare our method and *baseline 1,2* with key metrics in various scenarios in the CARLA simulator and real world. All scenario in Fig.6 are evaluated in the simulator and scenario 1 and 5 in Fig.6 are evaluated in real world. In the simulator, each scenario is simulated 500 times with different kinds of vehicles of which velocity is random between $[v_{road_speed_limit}, 1.5 \times v_{road_speed_limit}]$ and the speed of pedestrian is also set as random between $[4km/h, 6km/h]$. In real world, each scenario was evaluated 10 times with random velocity of occluded agents. The proposed method was implemented with AMD Ryzen 7 series clocked at 2.2 GHz.

A. Baseline Methods

1) Baseline 1: The *Baseline 1* used *Path Velocity Decomposition* method without occlusion risk assessment. The path is given by the route of the ego-vehicle, and the velocity profile is generated using PJSO [21].

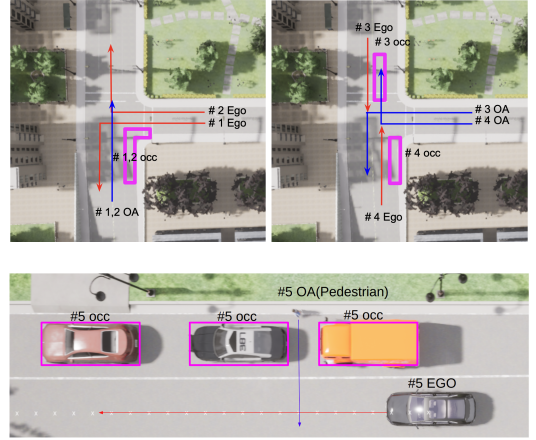


Fig. 6: Illustration of five scenarios in CARLA simulator. Obstacles that induce occlusion is represented as a magenta polygon. The ego vehicle drives along the route(red arrow) and come across occluded agents(OA) moving along its route(blue arrow).

2) Baseline 2: The *baseline 2* is *baseline 1* with the SOTA occlusion risk assessment algorithm proposed in [5]. Compare to *baseline 2*, the strength of our method is robustness in various scenarios(including occluded pedestrians scenarios) and computational efficiency. Yet the result of assessing the occlusion risk of PV is similar and [5] can't be used in occluded pedestrian scenarios, so we only compare total computation time of planning stack in scenarios without occluded pedestrians. Since *baseline 2* and our method uses the same planning strategy(*baseline 1*), computation time is fairly compared.

B. Metrics

There are four metrics to evaluate the methods. 1) discomfort score, 2) collision rate, 3) traversal time, 4) computation time. The discomfort score and collision rate is defined as follows:

1) Discomfort score: We use the discomfort score defined in [5] to represent the discomfort of passengers in the ego-vehicle.

$$\text{Discomfort Score} = \frac{1}{T} \int_0^T \max(0, |a_{ego}(t)| - a_{thresh}) dt$$

2) Collision Rate: Collision rate is defined simply the number of simulations with collision divided by the total number of simulations.

$$\text{Collision Rate} = \frac{\# \text{ of simulations with collision}}{\text{Total } \# \text{ of simulations}} \times 100\%$$

VI. RESULT

Our proposed algorithm showed 'Collision Rate' decreased up to $6.14\times$, 'Discomfort Score' decreased up to $5.03\times$, and the lowest increase in 'Traversal Time' is $1.48\times$ compared to *baseline 1*. The overall result is presented in Table.I. In Table.I, scenario 3,4 has resulted better than scenario 1,2. The reason is that the route path of the ego vehicle in scenario 1,2 includes left/right turn, which makes

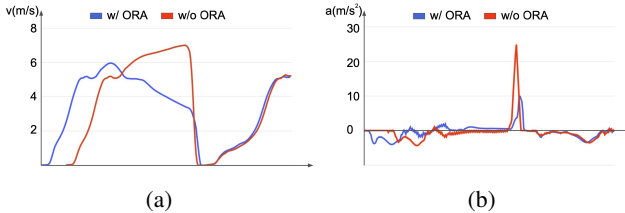


Fig. 7: (a) v-t graph and (b) a-t(deceleration) graph of baseline 1(blue) and our method(red) in a scenario.

Evaluation Table			
Scenario	collision rate	discomfort score	traversal time
1 Baseline1 ORA	15.8%	0.0663	14.22s
	6.00%	0.0251	20.63s
2 Baseline1 ORA	0.600%	0.000854	15.00s
	0.200%	0.000779	16.82s
3 Baseline1 ORA	3.00 × DEC	1.10 × DEC	1.12 × INC
	8.60%	0.00471	8.75s
4 Baseline1 ORA	1.4%	0.000937	12.97s
	6.14 × DEC	5.03 × DEC	1.48 × INC
5 Baseline1 ORA	1.20%	0.00202	11.1s
	0.400%	0.000444	17.4s
cf	3.00 × DEC	4.54 × DEC	1.56 × INC
	24.0%	0.0186	12.58s
Baseline1 ORA	10.0%	0.00650	13.78s
	2.40 × DEC	2.86 × DEC	1.10 × INC

TABLE I: Table of comparing metrics of ORA(Our method) and Baseline1

Computation Time Table				
Scenario #	1	2	3	4
Baseline2	26.2528ms	18.6865ms	32.0241ms	39.9024ms
ORA	1.3029 ms	1.5005 ms	1.6467 ms	2.6913 ms
cf	20.15×DEC	12.45×DEC	19.45×DEC	14.83×DEC

TABLE II: Table of comparing average computation time ORA(Our method) and Baseline2

the ego vehicle slow down before the speed limit due to occlusion. Therefore difference of velocity profile between w/ and w/o our method becomes unclear. In Fig.7 v-t and a-t(deceleration) graphs of an episode of scenario 1 in the simulator are shown. *Baseline 1* and our method both managed to safely stop and avoid collision with a suddenly appearing vehicle. However, our method has reduced the velocity before entering the intersection and prevented itself from sudden deceleration and collision.

We have compared the average 'Computation Time' of *baseline 2* with our method in various scenarios. Even though we set *baseline 2* to have a number of particles $N_k \leq 4 \cdot 10^4$ which was much smaller than it was used for evaluation in [5], we have reduced 'Computation Time' up to $20.15 \times$ compared to *baseline 2* due to our novel *Simplified Reachability Quantification*. The overall average computation time result is in Table.II:

VII. CONCLUSION AND FUTURE WORK

We proposed the occlusion-aware risk assessment method and planning strategy using *Simplified Reachability Quantification*. We have improved the work of [3]–[5], [9] by proposing *Simplified Reachability Quantification*, node clas-

sification and extending it to risk assessment of occluded pedestrians. Our method is evaluated in various scenarios through the CARLA simulator, and compared with *baseline 1,2* methods. The result showed that our method effectively decreased collision rate and discomfort score in arbitrary scenarios while using much less computation time than *baseline 2*.

Future works will be removing redundant phantom agents by sequential reasoning. Reasoning observation over time could prevent the ego vehicle from being conservative and make its driving efficient.

APPENDIX

This appendix proves a *Simplified Reachability Quantification* We aim to quantify the PVs that could reach the collision point using BRS. Then, we will define it as an occlusion risk.

Given T_{pred} , DPVS, maximum velocity of PV v_{max} and the scenario illustrated in Fig.3, let the x an initial position of a PV, the y a final position of a PV, the $f(y)$ amount of PV that could reach the y . We assume that PV drives along the centerline therefore x and y are *simply* longitudinal positions in the Frenet frame of PV. The PV could be at a random position in DPVS with random velocity. However, with no prior given, we have chosen to assume that the PV is uniformly distributed and moves in constant velocity that are uniformly distributed like [5] did.

The function $f(y)$ is defined in three parts by the value of y . The intervals are $I_1 := [s_s, s_e]$, $I_2 := [s_e, s_e + v_{max}T_{pred}]$, $I_3 := [s_e + v_{max}T_{pred}, s_e + v_{max}T_{pred}]$. Note that $s_e - s_s \leq v_{max}T_{pred}$ always satisfies by definition of DPVS in IV-B.

In Fig.8, the PVs that could reach the y and satisfy the conditions are represented in a gray-shaded area. Since we assumed that the initial position and velocity of PVs are uniformly distributed, simply the area of the gray shaded area represents the PVs that could reach the y . Note that $x \in [s_s, s_e]$, $v \in [0, v_{max}]$, $t \in [0, T_{pred}]$ conditions should be satisfied.

To intuitively understand Fig.8, the blue line represents the PVs that initial positions are already in y , so they reach the y in $t = 0$ regardless of their velocities, and the red line represents the PVs that manage to reach the y in $t = T_{pred}$.

Since we assumed that every PV moves in a constant velocity, $y = x + vt$ always satisfies. Using this condition, $f(y)$ is easily driven. For convenience, we used s instead of y since the meaning of the $f(y)$ is occlusion risk in the Frenet frame's longitudinal position s . Its graph is illustrated in Fig.9 and derived as follows:

$$f(s)$$

$$:= \begin{cases} \frac{1}{2}(2v_{max} - \frac{s-s_s}{T_{pred}})(s-s_s), & s \in I_1 \\ \frac{1}{2}(2v_{max} - \frac{s-s_s}{T_{pred}} - \frac{s-s_e}{T_{pred}})(s_e-s_s), & s \in I_2 \\ \frac{1}{2}(v_{max} - \frac{s-s_e}{T_{pred}})(s_e - (s - v_{max}T_{pred})), & s \in I_3 \end{cases} \quad (14)$$

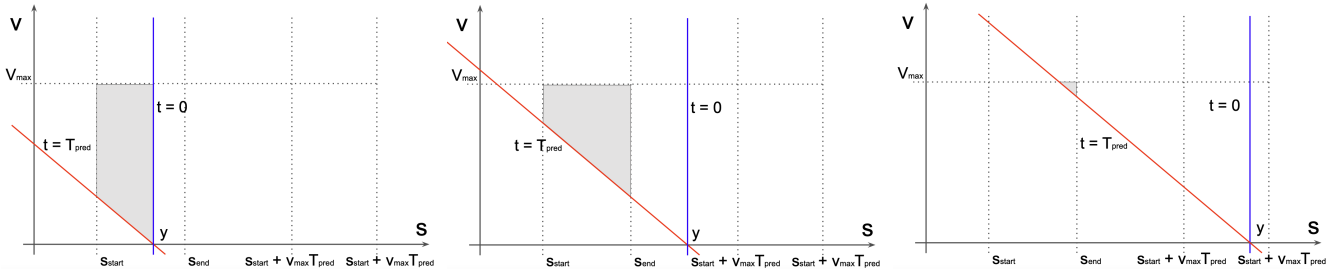


Fig. 8: The gray shaded area represents the $f(y)$. Each graphs are illustrated depending on the value of y .

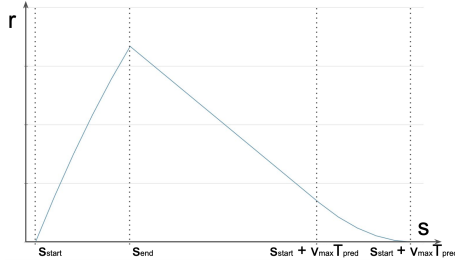


Fig. 9: Occlusion risk due to DPVS is represented.

REFERENCES

[1] Pongsathorn Raksincharoensak, Takahiro Hasegawa, and Masao Nagai. Motion planning and control of autonomous driving intelligence system based on risk potential optimization framework. *International Journal of Automotive Engineering*, 7(AVEC14):53–60, 2016.

[2] Shane Gilroy, Edward Jones, and Martin Glavin. Overcoming occlusion in the automotive environment—a review. *IEEE Transactions on Intelligent Transportation Systems*, 22(1):23–35, 2019.

[3] Markus Koschi and Matthias Althoff. Set-based prediction of traffic participants considering occlusions and traffic rules. *IEEE Transactions on Intelligent Vehicles*, 6(2):249–265, 2020.

[4] Ming-Yuan Yu, Ram Vasudevan, and Matthew Johnson-Roberson. Risk assessment and planning with bidirectional reachability for autonomous driving. In *2020 IEEE International Conference on Robotics and Automation (ICRA)*, pages 5363–5369. IEEE, 2020.

[5] Ming-Yuan Yu, Ram Vasudevan, and Matthew Johnson-Roberson. Occlusion-aware risk assessment for autonomous driving in urban environments. *IEEE Robotics and Automation Letters*, 4(2):2235–2241, 2019.

[6] Stephen G McGill, Guy Rosman, Teddy Ort, Alyssa Pierson, Igor Gilitschenski, Brandon Araki, Luke Fletcher, Sertac Karaman, Daniela Rus, and John J Leonard. Probabilistic risk metrics for navigating occluded intersections. *IEEE Robotics and Automation Letters*, 4(4):4322–4329, 2019.

[7] Minchul Lee, Kichun Jo, and Myoungcho Sunwoo. Collision risk assessment for possible collision vehicle in occluded area based on precise map. In *2017 IEEE 20th International Conference on Intelligent Transportation Systems (ITSC)*, pages 1–6. IEEE, 2017.

[8] Lingguang Wang, Carlos Fernandez Lopez, and Christoph Stiller. Generating efficient behaviour with predictive visibility risk for scenarios with occlusions. In *2020 IEEE 23rd International Conference on Intelligent Transportation Systems (ITSC)*, pages 1–7. IEEE, 2020.

[9] Piotr F Orzechowski, Annika Meyer, and Martin Lauer. Tackling occlusions & limited sensor range with set-based safety verification. In *2018 21st International Conference on Intelligent Transportation Systems (ITSC)*, pages 1729–1736. IEEE, 2018.

[10] Yannik Nager, Andrea Censi, and Emilio Frazzoli. What lies in the shadows? safe and computation-aware motion planning for autonomous vehicles using intent-aware dynamic shadow regions. In *2019 International Conference on Robotics and Automation (ICRA)*, pages 5800–5806. IEEE, 2019.

[11] José Manuel Gaspar Sánchez, Truls Nyberg, Christian Pek, Jana Tumova, and Martin Törngren. Foresee the unseen: Sequential reasoning about hidden obstacles for safe driving. In *2022 IEEE Intelligent Vehicles Symposium (IV)*, pages 255–264. IEEE, 2022.

[12] Kristijan Macek, Díaz Alejandro Vasquez Govea, Thierry Fraichard, et al. Towards safe vehicle navigation in dynamic urban scenarios. *Automatika-Journal for Control, Measurement, Electronics, Computing and Communications*, 2009.

[13] Sara Bouraine, Thierry Fraichard, and Hassen Salhi. Provably safe navigation for mobile robots with limited field-of-views in dynamic environments. *Autonomous Robots*, 32:267–283, 2012.

[14] Shai Shalev-Shwartz, Shaked Shammah, and Amnon Shashua. On a formal model of safe and scalable self-driving cars. *arXiv preprint arXiv:1708.06374*, 2017.

[15] Christian Pek and Matthias Althoff. Computationally efficient fail-safe trajectory planning for self-driving vehicles using convex optimization. In *2018 21st International Conference on Intelligent Transportation Systems (ITSC)*, pages 1447–1454. IEEE, 2018.

[16] Matthias Althoff and Silvia Magdici. Set-based prediction of traffic participants on arbitrary road networks. *IEEE Transactions on Intelligent Vehicles*, 1(2):187–202, 2016.

[17] M Sadou, V Polotski, and P Cohen. Occlusions in obstacle detection for safe navigation. In *IEEE Intelligent Vehicles Symposium, 2004*, pages 716–721. IEEE, 2004.

[18] Maximilian Naumann, Hendrik Konigshof, Martin Lauer, and Christoph Stiller. Safe but not overcautious motion planning under occlusions and limited sensor range. In *2019 IEEE Intelligent Vehicles Symposium (IV)*, pages 140–145. IEEE, 2019.

[19] Maxime Bouton, Alireza Nakhaei, Kikuo Fujimura, and Mykel J Kochenderfer. Scalable decision making with sensor occlusions for autonomous driving. In *2018 IEEE international conference on robotics and automation (ICRA)*, pages 2076–2081. IEEE, 2018.

[20] Moritz Werling, Julius Ziegler, Sören Kammler, and Sebastian Thrun. Optimal trajectory generation for dynamic street scenarios in a frenet frame. In *2010 IEEE International Conference on Robotics and Automation*, pages 987–993. IEEE, 2010.

[21] Jinyun Zhou, Runxin He, Yu Wang, Shu Jiang, Zhenguang Zhu, Jiangtao Hu, Jinghao Miao, and Qi Luo. Autonomous driving trajectory optimization with dual-loop iterative anchoring path smoothing and piecewise-jerk speed optimization. *IEEE Robotics and Automation Letters*, 6(2):439–446, 2020.